Tuning of Optical Band Gaps: Syntheses, Structures, Magnetic Properties, and Optical Properties of CsLnZnSe 3 (Ln = Sm, Tb, Dy, Ho, Er, Tm, Yb, and Y)

ARTICLE *in* INORGANIC CHEMISTRY · APRIL 2002

Impact Factor: 4.76 · DOI: 10.1021/ic011200u · Source: PubMed

5 AUTHORS, INCLUDING:

Christy Haynes
University of Minnesota Twin Cities
140 PUBLICATIONS **8,890** CITATIONS

SEE PROFILE

Inorg. Chem. **2002**, *41*, 1199–1204

Tuning of Optical Band Gaps: Syntheses, Structures, Magnetic Properties, and Optical Properties of $CsLnZnSe_3$ (Ln = Sm, Tb, Dy, Ho, Er, Tm, Yb, and Y)

Kwasi Mitchell, Christy L. Haynes, Adam D. McFarland, Richard P. Van Duyne, and James A. Ibers*

Department of Chemistry, Northwestern University, 2145 Sheridan Road, Evanston, Illinois 60208

Received November 26, 2001

Eight new quaternary selenides $CsSmZnSe_3$, $CsTbZnSe_3$, $CsDyZnSe_3$, $CsHoZnSe_3$, $CsErZnSe_3$, $CsTmZnSe_3$, $CsYbZnSe_3$, and $CsYZnSe_3$ have been synthesized with the use of high-temperature solid-state experimental methods. These compounds are isostructural with $KZrCuS_3$, crystallizing with four formula units in the orthorhombic space group *Cmcm*. The structure of these $CsLnZnSe_3$ compounds is composed of $^2_\infty[LnZnSe_3^-]$ layers separated by Cs atoms. The Ln atom is octahedrally coordinated by six Se atoms, the Zn atom is tetrahedrally coordinated by four Se atoms, and the Cs atom is coordinated by a bicapped trigonal prism of eight Se atoms. Because there are no Se–Se bonds in the structure, the oxidation state of Cs is 1+, that of Ln is 3+, and that of Zn is 2+. $CsYbZnSe_3$ exhibits an antiferromagnetic transition at 11 K, whereas $CsSmZnSe_3$ does not follow a Curie–Weiss law. The remaining rare-earth compounds are paramagnetic, and the calculated effective magnetic moments of the rare-earth ions agree well with their theoretical values. Optical absorption data on face-indexed single crystals of $CsSmZnSe_3$, $CsErZnSe_3$, $CsYbZnSe_3$, and $CsYZnSe_3$ demonstrate that the optical band gap changes by more than 0.75 eV with the composition and by as much as 0.20 eV with the crystal orientation. The optical band gaps range from 2.63 eV ($CsSmZnSe_3$, $CsErZnSe_3$) to 1.93 eV ($CsYbZnSe_3$) for the (010) crystal face and 2.56 eV ($CsErZnSe_3$) to 1.88 eV ($CsYbZnSe_3$) for the (001) crystal face. The difference in the optical band gap of the (010) face vs the (001) face varies from +0.05 eV ($CsYbZnSe_3$) to +0.20 eV ($CsSmZnSe_3$).

Introduction

The reactive flux method[1] has been employed successfully over the past several years to synthesize a variety of quaternary alkali-metal rare-earth d-element chalcogenides (A/Ln/M/Q). The d-element in these systems predominantly has been a coinage metal. These materials display a variety of layered and tunnel structure types in addition to interesting physical properties. Examples include $RbLn_2CuSe_4$ (Ln = Sm, Gd, Dy),[2] $Rb_{1.5}Ln_2Cu_{2.5}Se_5$ (Ln = Gd, Dy),[2] $RbSm_2Ag_3Se_5$,[2] $BaLnMQ_3$ (Ln = rare earth; M = Cu, Ag, Au; Q = S, Se, Te),[3−6] $Ba_2LnAg_5S_6$ (Ln = La, Y),[7] KGd_2CuS_4,[8] $K_2CeCu_2S_4$,[9] $ALnCu_2S_6$ (A = K, Cs; Ln = La, Ce, Eu),[9−11] $K_{1.5}Dy_2Cu_{2.5}Te_5$,[6] $K_{0.5}Ba_{0.5}DyCu_{1.5}Te_3$,[6] $ALnCuQ_3$ (A = K, Cs; Ln = Ce, Th, U; Q = S, Se, Te),[11,12] $K_2CeAg_3Te_4$,[13] $KCeCuTe_4$,[14] and $Rb_2CeCu_3Te_5$.[15]

Recently, the reactive flux method was used to synthesize the ivory-colored semiconductor $CsGdZnSe_3$.[16] This compound possesses the layered $KZrCuS_3$ structure type,[17] which

* Author to whom correspondence should be addressed. E-mail: ibers@chem.northwestern.edu.

(1) Sunshine, S. A.; Kang, D.; Ibers, J. A. *J. Am. Chem. Soc.* **1987**, *109*, 6202−6204.
(2) Huang, F. Q.; Ibers, J. A. *J. Solid State Chem.* **2000**, *151*, 317−322.
(3) Christuk, A. E.; Wu, P.; Ibers, J. A. *J. Solid State Chem.* **1994**, *110*, 330−336.
(4) Wu, P.; Christuk, A. E.; Ibers, J. A. *J. Solid State Chem.* **1994**, *110*, 337−344.
(5) Wu, P.; Ibers, J. A. *J. Alloys Compd.* **1995**, *229*, 206−215.
(6) Huang, F. Q.; Choe, W.; Lee, S.; Chu, J. S. *Chem. Mater.* **1998**, *10*, 1320−1326.
(7) Wu, P.; Ibers, J. A. *Z. Kristallogr.* **1993**, *208*, 35−41.
(8) Stoll, P.; Dürichen, P.; Näther, C.; Bensch, W. *Z. Anorg. Allg. Chem.* **1998**, *624*, 1807−1810.
(9) Sutorik, A. C.; Albritton-Thomas, J.; Kannewurf, C. R.; Kanatzidis, M. G. *J. Am. Chem. Soc.* **1994**, *116*, 7706−7713.
(10) Bensch, W.; Dürichen, P. *Chem. Ber.* **1996**, *129*, 1489−1492.
(11) Sutorik, A. C.; Albritton-Thomas, J.; Hogan, T.; Kannewurf, C. R.; Kanatzidis, M. G. *Chem. Mater.* **1996**, *8*, 751−761.
(12) Cody, J. A.; Ibers, J. A. *Inorg. Chem.* **1995**, *34*, 3165−3172.
(13) Patschke, R.; Brazis, P.; Kannewurf, C. R.; Kanatzidis, M. *Inorg. Chem.* **1998**, *37*, 6562−6563.
(14) Patschke, R.; Heising, J.; Kanatzidis, M. *Chem. Mater.* **1998**, *10*, 695−697.
(15) Patschke, R.; Brazis, P.; Kannewurf, C. R.; Kanatzidis, M. *J. Mater. Chem.* **1998**, *8*, 2587−2589.
(16) Huang, F. Q.; Mitchell, K.; Ibers, J. A. *Inorg. Chem.* **2001**, *40*, 5123−5126.

10.1021/ic011200u CCC: $22.00
Published on Web 02/12/2002

Table 1. Crystal Data and Structure Refinements for $CsLnZnSe_3$[a]

	$CsSmZnSe_3$	$CsTbZnSe_3$	$CsDyZnSe_3$	$CsHoZnSe_3$	$CsErZnSe_3$	$CsTmZnSe_3$	$CsYbZnSe_3$	$CsYZnSe_3$
fw	585.51	594.08	597.66	600.09	602.42	604.09	608.20	524.07
a, Å	4.1935(14)	4.1514(6)	4.1282(9)	4.1275(5)	4.1166(6)	4.104(3)	4.0853(4)	4.1409(4)
b, Å	15.753(5)	15.785(2)	15.767(4)	15.814(2)	15.816(2)	15.825(13)	15.7864(15)	15.8145(15)
c, Å	11.102(4)	10.9634(15)	10.910(3)	10.8974(14)	10.8574(17)	10.818(9)	10.8068(10)	10.9284(11)
V, Å^3	733.4(4)	718.42(17)	710.1(3)	711.28(15)	706.91(19)	702.6(10)	696.95(11)	715.66(12)
ρ_c, gcm^{-3}	5.303	5.493	5.590	5.604	5.660	5.711	5.796	4.864
μ, cm^{-1}	308.52	331.67	341.17	346.81	355.75	364.74	374.60	315.62
$R(F)$[b]	0.0275	0.0247	0.0270	0.0277	0.0274	0.0220	0.0288	0.0225
$R_w(F^2)$[c]	0.0663	0.0678	0.0675	0.0754	0.0743	0.0635	0.0751	0.0677

[a] For all structures $Z = 4$, space group = *Cmcm*, $T = 153(2)$ K, and $\lambda = 0.71073$ Å. [b] $R(F) = \sum||F_o| - |F_c||/\sum|F_o|$ for $F_o^2 > 2\sigma(F_o^2)$. [c] $R_w(F^2) = \{\sum[w(F_o^2 - F_c^2)^2]/\sum wF_o^4\}^{1/2}$ for all data. $w^{-1} = \sigma^2(F_o^2) + (0.04F_o^2)^2$ for $F_o^2 \geq 0$ and $w^{-1} = \sigma^2(F_o^2)$ for $F_o^2 < 0$.

Table 2. Selected Bond Lengths (Å) for $CsLnZnSe_3$

	$CsSmZnSe_3$	$CsTbZnSe_3$	$CsDyZnSe_3$	$CsHoZnSe_3$	$CsErZnSe_3$	$CsTmZnSe_3$	$CsYbZnSe_3$	$CsYZnSe_3$
Cs−Se1 × 4	3.6830(10)	3.6845(7)	3.6793(9)	3.6885(8)	3.6884(9)	3.6876(19)	3.6837(8)	3.6912(6)
Cs−Se1 × 2	3.9493(13)	3.8951(8)	3.8765(10)	3.8702(8)	3.8558(9)	3.844(3)	3.8387(9)	3.8798(6)
Cs−Se2 × 2	3.6004(13)	3.5996(10)	3.5897(12)	3.5998(11)	3.6003(12)	3.598(2)	3.5856(12)	3.6049(8)
Ln-Se1 × 4	2.9079(8)	2.8747(5)	2.8573(7)	2.8561(6)	2.8464(6)	2.8368(17)	2.8209(6)	2.8652(4)
Ln−Se2 × 2	2.9065(9)	2.8729(5)	2.8606(7)	2.8575(5)	2.8473(5)	2.839(2)	2.8368(4)	2.8641(3)
Zn−Se1 × 2	2.4380(11)	2.4357(9)	2.4331(10)	2.4354(9)	2.4324(10)	2.4320(18)	2.4337(10)	2.4371(7)
Zn−Se2 × 2	2.5750(11)	2.5588(9)	2.5464(11)	2.5514(10)	2.5472(11)	2.5413(18)	2.5292(11)	2.5571(7)

has three different crystallographically distinct sites over which cations may order (tetrahedral, octahedral, and bicapped trigonal prismatic). The structure is an ideal one for assessing the effect of chemical substitution on physical properties. The present investigation details the synthesis, structure, magnetic, and optical properties of eight new quaternary chalcogenides in the $CsLnZnSe_3$ series, namely, $CsSmZnSe_3$, $CsTbZnSe_3$, $CsDyZnSe_3$, $CsHoZnSe_3$, $CsErZnSe_3$, $CsTmZnSe_3$, $CsYbZnSe_3$, and $CsYZnSe_3$. These compounds, which have the simple $KZrCuS_3$ structure type,[17] represent a new class of transparent, magnetic semiconductors whose optical band gap may be controlled by means of chemical substitution and crystal orientation.

Experimental Section

Syntheses. The following reagents were used as obtained: Cs (Aldrich, 99.5%), Sm (Alfa Aesar, 99.9%), Tb (Alfa Aesar, 99.9%), Dy (Alfa Aesar, 99.9%), Ho (Alfa Aesar, 99.9%), Er (Strem, 99.9%), Tm (Strem, 99.9%), Yb (Strem, 99.9%), Y (Alfa Aesar, 99.9%), Zn (Johnson Matthey, 99.99%), Se (Aldrich, 99.5%), and CsI (Aldrich, 99.99%). Cs_2Se_3, the reactive flux[1] employed in the syntheses, was prepared by the stoichiometric reaction of the elements in liquid NH_3. Reaction mixtures of 0.3 mmol of Cs_2Se_3, 0.5 mmol of Ln, 0.5 mmol of Zn, 1.0 mmol of Se, and approximately 150 mg of CsI (used to aid crystal growth) were loaded into fused-silica tubes under an Ar atmosphere in a glovebox. These tubes were sealed under a 10^{-4} Torr atmosphere and then placed in a computer-controlled furnace. The samples were heated to 1273 K in 48 h, kept at 1273 K for 50 h, and cooled at 4 K/h to 473 K, and then the furnace was turned off. The reaction mixtures were washed with *N*,*N*-dimethylformamide and water and finally dried with acetone. In each reaction, transparent, colored needles and plates of $CsLnZnSe_3$ were obtained in nearly quantitative yield, based upon Ln. The colors of the crystals include yellow ($CsSmZnSe_3$), pale yellow ($CsTbZnSe_3$, $CsHoZnSe_3$, $CsErZnSe_3$, $CsYZnSe_3$), gray ($CsDyZnSe_3$, $CsTmZnSe_3$), and red ($CsYbZnSe_3$). All of the products were consistent with the stated compositions, as determined by the examination of selected single crystals with an EDX-equipped Hitachi S-3500 SEM. The compounds are moderately stable in air.

Structure Determinations. Single-crystal X-ray diffraction data were collected with the use of graphite-monochromatized Mo Kα radiation ($\lambda = 0.71073$ Å) at 153 K on a Bruker Smart-1000 CCD diffractometer.[18] The crystal-to-detector distance was 5.023 cm. Crystal decay was monitored by re-collecting 50 initial frames at the end of data collection. Data were collected by a scan of 0.3° in ω in groups of 606, 606, 606, and 606 frames at ϕ settings of 0°, 90°, 180°, and 270° for $CsSmZnSe_3$, $CsTbZnSe_3$, $CsHoZnSe_3$, $CsErZnSe_3$, $CsTmZnSe_3$, and $CsYZnSe_3$, and in groups of 606, 606, and 606 frames at ϕ settings of 0°, 120°, and 240° for $CsDyZnSe_3$ and $CsYbZnSe_3$. The exposure times varied from 9 to 20 s/frame. The collection of the intensity data was carried out with the program SMART.[18] Cell refinement and data reduction were carried out with the use of the program SAINT,[18] and face-indexed absorption corrections were performed numerically with the use of the program XPREP.[19] Then the program SADABS[18] was employed to make incident beam and decay corrections.

The structures were solved with the direct methods program SHELXS and refined with the full-matrix least-squares program SHELXL of the SHELXTL.PC suite of programs.[19] Each final refinement included anisotropic displacement parameters and a secondary extinction correction. Additional experimental details are shown in Table 1 and in the Supporting Information. Table 2 presents selected bond distances.

Magnetic Susceptibility Measurements. These measurements on $CsSmZnSe_3$ (79.0 mg), $CsTbZnSe_3$ (73.3 mg), $CsDyZnSe_3$ (63.6 mg), $CsHoZnSe_3$ (47.5 mg), $CsErZnSe_3$ (79.5 mg), $CsTmZnSe_3$ (55.7 mg), and $CsYbZnSe_3$ (69.4 mg) were carried out with the use of a Quantum Design SQUID magnetometer (MPMS5 Quantum Design). The composition of each sample was verified by EDX measurements. All samples were ground and loaded into gelatin capsules. Zero-field cooled (ZFC) susceptibility data were collected between 5 and 300 K. The applied field was 100 G. All measurements were corrected for core diamagnetism.[20] The susceptibility data in the temperature range 100−300 K were fit by a

(17) Mansuetto, M. F.; Keane, P. M.; Ibers, J. A. *J. Solid State Chem.* **1992**, *101*, 257−264.
(18) *SMART Version 5.054 Data Collection* and *SAINT-Plus Version 6.02A Data Processing Software for the SMART System*; Bruker Analytical X-Ray Instruments, Inc.: Madison, WI, 2000.
(19) Sheldrick, G. M. *SHELXTL DOS/Windows/NT*, version 5.10; Bruker Analytical X-Ray Instruments, Inc.: Madison, WI, 1997.

Table 3. Magnetic Properties of $CsLnZnSe_3$

compound	C (emu K mol^{-1})	θ_p (K)	μ_{eff} (μ_B) obs	μ_{eff} (μ_B) theory[a]
$CsTbZnSe_3$	12.30(2)	−19.6(3)	9.92(2)	9.5
$CsDyZnSe_3$	15.04(1)	−11.9(2)	10.97(1)	10.63
$CsHoZnSe_3$	13.92(1)	−6.3(1)	10.55(1)	10.60
$CsErZnSe_3$	11.24(1)	−6.72(5)	9.48(1)	9.59
$CsTmZnSe_3$	7.79(2)	−25.6(7)	7.84(2)	7.57
$CsYbZnSe_3$	2.69(1)	−50.2(2)	4.64(2)	4.54

[a] Reference 30.

least-squares method to the Curie−Weiss equation $\chi = C/(T - \theta_p)$, where C is the Curie constant and θ_p is the Weiss constant. The effective magnetic moment (μ_{eff}) was calculated from the equation $\mu_{eff} = (7.997C)^{1/2}\mu_B$.[21] The resulting values for C, θ_p, and μ_{eff} are summarized in Table 3.

Optical Microspectroscopy Measurements. Selected single crystals of the $CsLnZnSe_3$ compounds were face-indexed and their dimensions were measured by means of the video attachment of a Bruker Smart-1000 CCD diffractometer.[18] Crystal dimensions were as follows ([100], [010], [001]): $CsSmZnSe_3$ 470, 35, 83 μm; $CsErZnSe_3$ 293, 20, 41 μm; $CsYbZnSe_3$ 380, 83, 76 μm; $CsYZnSe_3$ 500, 32, 50 μm. Absorption measurements on these single crystals with unpolarized light were performed with the use of an Ocean Optics model SD2000 spectrometer over the range 450 nm (2.76 eV) to 1000 nm (1.24 eV) at 293 K. The spectrometer was coupled by fiber optics to a modified Nikon Optiphot microscope. A tungsten−halogen lamp (Ocean Optics, model LS-1-LL) was coupled to the microscope with a 400 μm core diameter input fiber. The light exiting the fiber was collimated by means of a gradient index lens assembly (Thorlabs), and the beam was expanded with the use of a home-built, variable power beam expander to fill the microscope objective (20X ELWD, NA = 0.4, Nikon). A spherical mirror (f = 12.5 mm, diameter = 30 mm, Melles Griot) was placed under the objective so that the center of curvature of the mirror was coincident with the focal point of the objective lens. The light reflected off the spherical mirror was recollimated by the objective lens before being focused into the 400 μm core diameter fiber coupled to the spectrometer. Fine alignment of the microscope assembly was achieved by maximizing the transmission of the source light. Crystals were positioned at the focal point of the objective by means of a goniometer mounted on translation stages (Line Tool Company). The rotation axis of the goniometer, which was coincident with the [100] crystal axis, was aligned perpendicular to the optical axis of the microscope so that the extinction spectra of the (010) and (001) crystal planes could be collected.

In order to account for incomplete filling of the probe spot size by some faces of the mounted single crystals, the absorption data were scaled with the use of the following formula:[22]

$$\eta = (2/(\pi D^2))[w(D^2 - w^2)^{1/2} + D^2 \arcsin(w/D)] \qquad (1)$$

where η is the fraction of the spot size filled by the crystal, w is the width of the crystal, and D is the white light probe diameter. The width was taken to be the separation of the (010) and (0$\bar{1}$0) or (001) and (00$\bar{1}$) faces when the (001) and (010) faces were measured, respectively. The scaled absorption value and the crystal thickness were then used to calculated the molar absorption coefficient (α) of each single-crystal sample. The band gap for these crystals was assumed to be a direct transition, and the data were manipulated accordingly. From α and the incident photon energy ($h\nu$), the direct band gap (E_g) for these semiconductors[23] was calculated according to the relation

$$(\alpha h\nu)^2 \sim h\nu - E_g \qquad (2)$$

from the extrapolation of a linear regression to $(\alpha h\nu)^2 = 0$ in a plot of $h\nu$ versus $(\alpha h\nu)^2$. These measurements and calculations were carried out for both the (010) and (001) faces of each of the materials (Table 4).

No f−f transitions appeared as dominant features in the recorded spectra.

Table 4. Optical Properties of $CsLnZnSe_3$

compound	cryst face	band gap (eV)	color
$CsSmZnSe_3$	(010)	2.63	bright yellow
	(001)	2.43	
$CsErZnSe_3$	(010)	2.63	pale yellow
	(001)	2.56	
$CsYbZnSe_3$	(010)	1.93	red
	(001)	1.88	
$CsYZnSe_3$	(010)	2.41	pale yellow
	(001)	2.29	

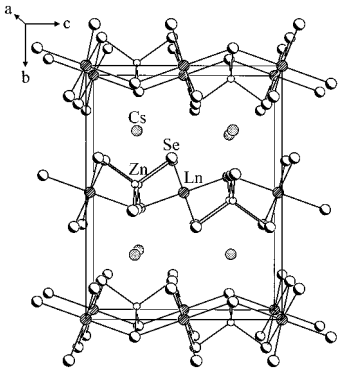

Figure 1. Unit cell of $CsLnZnSe_3$ viewed down [100].

Results and Discussion

The structure of the isostructural compounds $CsLnZnSe_3$ is illustrated in Figure 1. It is composed of two-dimensional $^2_\infty[LnZnSe_3^-]$ layers parallel to (101) separated by Cs atoms. The Cs atoms are coordinated to a bicapped trigonal prism of eight Se atoms. Each bicapped trigonal prism has two face-sharing neighbors along [100] and four edge-sharing ones along [001] to form a two-dimensional $^2_\infty[CsSe_3^{5-}]$ layer (Figure 2). The Ln atoms are coordinated to a slightly distorted octahedron of six Se atoms, whereas the Zn atoms are coordinated to a distorted tetrahedron of four Se atoms (Table 2). The $^2_\infty[LnZnSe_3^-]$ layer is constructed from these $LnSe_6$ octahedra and $ZnSe_4$ tetrahedra, as shown in Figure 3. The octahedra share edges (four Se1) in the [100] direction and vertices (two Se2) in the [001] direction to form a two-dimensional $^2_\infty[LnSe_3^{3-}]$ layer. These layers of octahedra are slightly buckled, giving rise to tetrahedral sites that are occupied by Zn atoms. Each $ZnSe_4$ tetrahedron links with

(20) Mulay, L. N.; Boudreaux, E. A., Eds. *Theory and Applications of Molecular Diamagnetism*; Wiley-Interscience: New York, 1976.
(21) O'Connor, C. J. *Prog. Inorg. Chem.* **1982**, *29*, 203−283.
(22) Altkorn, R.; Malinsky, M. D.; Van Duyne, R. P.; Koev, I. *Appl. Spectrosc.* **2001**, *55*, 373−381.
(23) Bang, T.-H.; Choe, S.-H.; Park, B.-N.; Jin, M.-S.; Kim, W.-T. *Semicond. Sci. Technol.* **1996**, *11*, 1159−1162.

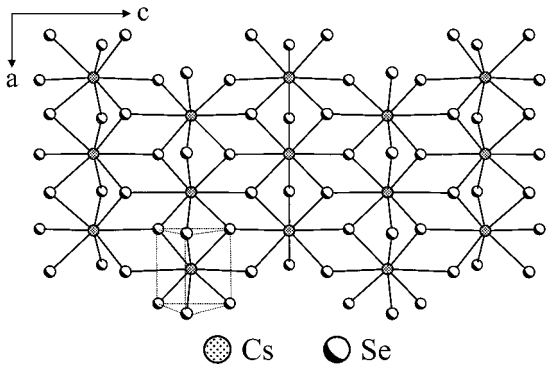

Figure 2. $^{2}_{\infty}[CsSe_3^{5-}]$ layer viewed down [010].

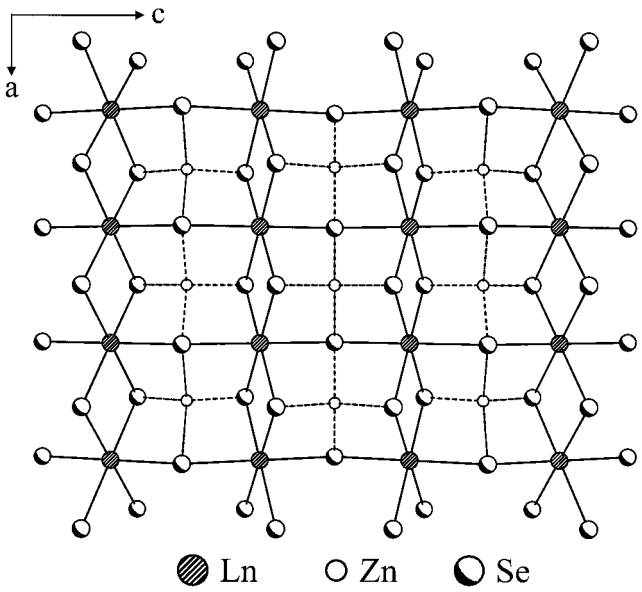

Figure 3. $^{2}_{\infty}[LnZnSe_3^{-}]$ layer viewed down [010].

four $LnSe_6$ octahedra by edge sharing along [001] to form the $^{2}_{\infty}[LnZnSe_3^{-}]$ layers.

Selected bond distances for $CsLnZnSe_3$ are displayed in Table 2. These bond lengths are normal. The ranges of distances are Sm−Se, 2.9065(9)−2.9079(8) Å; Tb−Se, 2.8729(5)−2.8747(5) Å; Dy−Se, 2.8573(7)−2.8606(7) Å; Ho−Se, 2.8561(6)−2.8575(5) Å; Er−Se, 2.8464(6)−2.8473(5) Å; Tm−Se, 2.8368(17)−2.839(2) Å; Yb−Se, 2.8209(6)−2.8368(4) Å; Y−Se, 2.8641(3)−2.8652(4) Å; Zn−Se, 2.4320(18)−2.5750(11) Å; Cs−Se, 3.5856(12)−3.9493(13) Å. These ranges are consistent, for example, with those of 2.8595(4)−3.0086(3) Å for Sm−Se in $CsSm_2CuSe_4$;[24] 2.8509(6)−2.9240(6) Å for Tb−Se in $CsTb_2Ag_3Se_5$;[24] 2.8218(12)−2.9385(8) Å for Dy−Se in $RbDy_2CuSe_4$;[2] 2.839(1) Å for Ho−Se in $CdHoSe_4$;[25] 2.770(2)−2.939(2) Å for Er−Se in $CsEr_3Se_5$;[26] 2.812(1) Å for Tm−Se in $CdTmSe_4$;[25] 2.752(3)−2.934(2) Å for Yb−Se in $Rb_3Yb_7Se_{12}$;[26] 2.879(1)−2.910(1) Å for Y−Se in $BaYAuSe_3$;[4] 3.4281(8)−3.9527(3) Å for Cs−Se in $CsSm_2CuSe_4$;[24] and the Zn−Se distance of 2.439(1) Å in $ZnGa_{0.4}Cr_{1.6}Se_4$.[27]

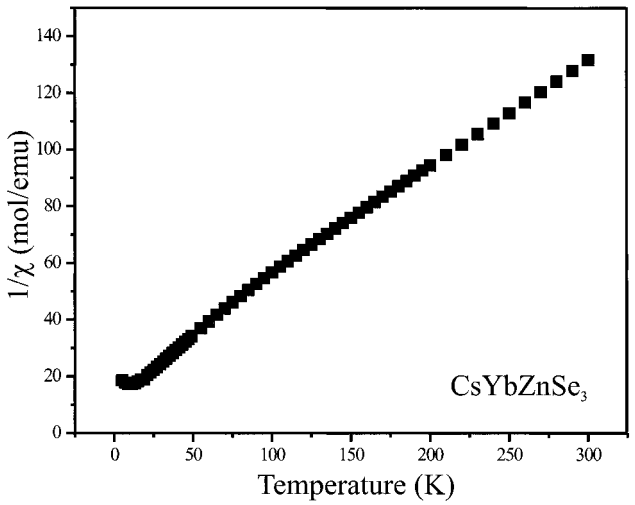

Figure 4. Plot of the inverse molar susceptibility ($1/\chi$) vs T for $CsYbZnSe_3$.

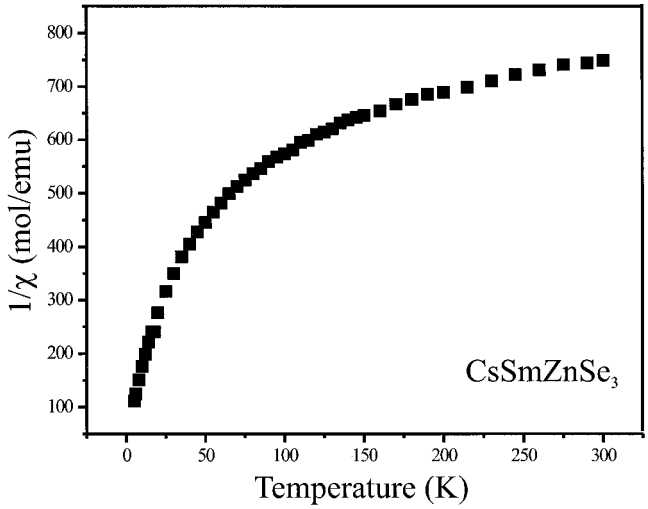

Figure 5. Plot of the inverse molar susceptibility ($1/\chi$) vs T for $CsSmZnSe_3$.

Because there are no Se−Se bonds in the structure of $CsLnZnSe_3$ the oxidation states of Cs/Ln/Zn/Se are 1+/3+/2+/2−. Several other isostructural compounds are known with the oxidation states A/Ln/M/Q of 1+ or 2+/3+ or 4+/1+/2−, such as $KZrCuQ_3$ (Q = S, Se, Te),[17] $CsUCuTe_3$,[12] $KUCuSe_3$,[11] $CsCeCuS_3$,[11] $TlZrCuTe_3$,[28] and $BaLnCuQ_3$ (Ln = rare earth, Y).[3,4,6] However, to the best of our knowledge the present $CsLnZnSe_3$ compounds are the only examples of quaternary alkali-metal rare-earth zinc chalcogenides known.

The plot of the reciprocal of the molar susceptibility ($1/\chi$) vs T for $CsYbZnSe_3$ is shown in Figure 4. $CsYbZnSe_3$ exhibits an antiferromagnetic transition at 11 K; however, above this transition temperature it is paramagnetic. Note that $CsTmZnSe_3$ does not exhibit an antiferromagnetic transition although the Tm^{3+} ions are 4.104(3) Å apart compared with a separation of 4.0853(4) Å for theYb^{3+} ions in $CsYbZnSe_3$. Additionally, the magnetic susceptibility of $CsSmZnSe_3$ does not follow a Curie−Weiss law (Figure 5)

(24) Huang, F. Q.; Ibers, J. A. *J. Solid State Chem.* **2001**, *158*, 299−306.
(25) Range, K.-J.; Eglmeier, C. *J. Alloys Compd.* **1991**, *176*, L13−L16.
(26) Kim, S.-J.; Park, S.-J.; Yun, H.; Do, J. *Inorg. Chem.* **1996**, *35*, 5283−5289.
(27) Okonska-Kozlowska, I.; Malicka, E.; Waskowska, A.; Mydlarz, T. *J. Solid State Chem.* **1999**, *148*, 215−219.
(28) Pell, M. A.; Ibers, J. A. *J. Alloys Compd.* **1996**, *240*, 37−41.

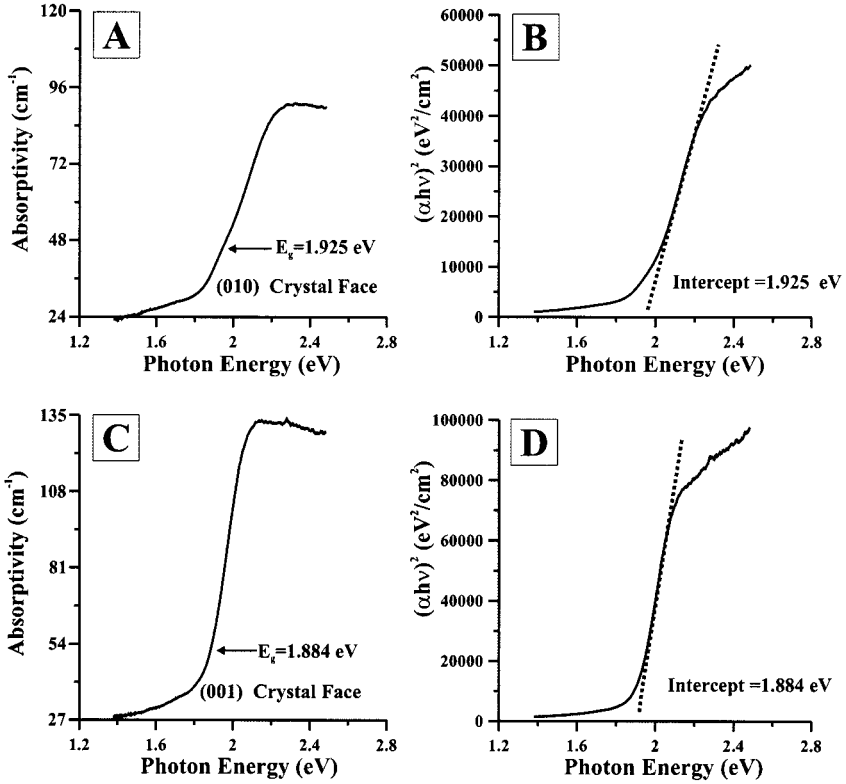

Figure 6. Optical absorption spectra and band gap calculation for the $CsYbZnSe_3$ crystal. Plots A and C show absorption spectra of (010) and (001) crystal faces, respectively, and B and D show plots of absorption data for the (010) and (001) faces, respectively.

because the effective moment of the 4f electrons has a temperature dependence that arises from low-lying multiplets.[29] All of the remaining $CsLnZnSe_3$ (Ln = Tb, Dy, Ho, Er, and Tm) compounds are paramagnetic over the range 5−300 K. The negative Weiss constant for these materials indicates that there is a small degree of local antiferromagnetic ordering. The calculated effective magnetic moments of all of the rare-earth ions agree well with their theoretical values (Table 3).[30]

The band gaps derived from the optical absorption spectra are tabulated for four of the present compounds in Table 4. The absorption edges of the remaining compounds were not entirely within the measurement range of the spectrometer used. We find a correlation of optical band gap (Table 4) with unit cell volume (Table 1). This correlation, which needs confirmation with additional data, is also seen in III−V and II−VI semiconductor materials.[31] The optical absorption spectra of the (010) and (001) crystal planes for $CsYbZnSe_3$ are depicted in Figure 6 along with the plots of $h\nu$ versus $(\alpha h\nu)^2$. The agreement between the raw data and the plots used for the band gap calculation justifies the assumption that the band gap for these crystals is a direct transition. It is evident from these data that the (010) crystal plane has a larger optical band gap than the (001) crystal plane. This observation is also true for $CsSmZnSe_3$, $CsErZnSe_3$, and $CsYZnSe_3$. Variation of the band gap with crystal orientation is expected, given that these materials crystallize in the orthorhombic system. Although this optical anisotropy of the $CsLnZnSe_3$ crystals has been demonstrated with the use of unpolarized light, it is probable that the use of polarized light, which we plan to utilize in future measurements, will provide more detailed information.[32,33]

It is clear that the $CsLnZnSe_3$ compounds offer flexibility in band gap engineering by control of composition and crystal orientation. From the present measurements (Table 4) we find that the optical band gap changes by more than 0.75 eV with composition and by as much as 0.20 eV with crystal orientation. The precise control of the optical band gap energy of a material is an important tool for the design of photonics devices, such as optical waveguides,[34] photon traps,[35] spontaneous emitters,[36] and optical filters.[37] Therefore, these $CsLnZnSe_3$ compounds are an interesting and potentially useful new class of optical materials. Given the stability and apparent broad range of the $KZrCuSe_3$ structure type, we expect further to tune the optical band gaps of new materials as we prepare additional compounds. Moreover, the combination of magnetic M species with magnetic Ln

(29) Van Vleck, J. H. *The Theory of Electric and Magnetic Susceptibilities*; Oxford University Press: London, 1932.
(30) Kittel, C. *Introduction to Solid State Physics*, 6th ed.; Wiley: New York, 1986.
(31) Solymar, L.; Walsh, D. *Electrical Properties of Materials*, 6th ed.; Oxford University Press: New York, 1998.
(32) Rau, J. W.; Kannewurf, C. R. *Phys. Rev. B* **1971**, *3*, 2581−2587.
(33) Ho, C. H.; Huang, Y. S.; Tiong, K. K.; Liao, P. C. *Phys. Rev. B: Condens. Matter* **1998**, *58*, 16130−16135.
(34) Joannopoulos, J. D.; Villeneuve, P. R.; Fan, S. *Nature (London)* **1997**, *386*, 143−149.
(35) Noda, S.; Chutinan, A.; Imada, M. *Nature (London)* **2000**, *407*, 608−610.
(36) Yablonovitch, E. *J. Opt. Soc. Am. B* **1993**, *10*, 283−295.
(37) Dirix, Y.; Bastiaansen, C.; Caseri, W.; Smith, P. *Adv. Mater.* **1999**, *11*, 223−227.

species will certainly lead to new compounds with interesting magnetic properties.

Acknowledgment. This research was supported by NSF Grant DMR00-96676, an IMGIP fellowship to K.M., and a GlaxoSmithKline sponsored ACS Division of Analytical Chemistry fellowship to C.L.H. Use was made of the Central Facilities supported by the MRSEC program of the National Science Foundation (DMR00-76097) at the Materials Research Center of Northwestern University.

Supporting Information Available: Crystallographic files in CIF format for $CsSmZnSe_3$, $CsTbZnSe_3$, $CsDyZnSe_3$, $CsHoZnSe_3$, $CsErZnSe_3$, $CsTmZnSe_3$, $CsYbZnSe_3$, and $CsYZnSe_3$. This material is available free of charge via the Internet at http://pubs.acs.org.

IC011200U